JACS
JOURNAL OF THE AMERICAN CHEMICAL SOCIETY

ARTICLE

pubs.acs.org/JACS

Aqueous Dispersion Polymerization: A New Paradigm for in Situ Block Copolymer Self-Assembly in Concentrated Solution

Shinji Sugihara,*[,†] Adam Blanazs,[‡] Steven P. Armes,*[,‡] Anthony J. Ryan,[‡] and Andrew L. Lewis[§]

[†]Department of Applied Chemistry and Biotechnology, Graduate School of Engineering, University of Fukui, 3-9-1 Bunkyo, Fukui 910-8507, Japan

[‡]Department of Chemistry, University of Sheffield, Dainton Building, Brook Hill, Sheffield, South Yorkshire S3 7HF, United Kingdom

[§]Biocompatibles UK Ltd., Chapman House, Farnham Business Park, Weydon Lane, Farnham, Surrey GU9 8QL, United Kingdom

Supporting Information

ABSTRACT: Reversible addition−fragmentation chain transfer polymerization has been utilized to polymerize 2-hydroxypropyl methacrylate (HPMA) using a water-soluble macromolecular chain transfer agent based on poly(2-(methacryloyloxy) ethylphosphorylcholine) (PMPC). A detailed phase diagram has been elucidated for this aqueous dispersion polymerization formulation that reliably predicts the precise block compositions associated with well-defined particle morphologies (i.e., pure phases). Unlike the ad hoc approaches described in the literature, this strategy enables the facile, efficient, and reproducible preparation of diblock copolymer spheres, worms, or vesicles directly in concentrated aqueous solution. Chain extension of the highly hydrated zwitterionic PMPC block with HPMA in water at 70 °C produces a hydrophobic poly(2-hydroxypropyl methacrylate) (PHPMA) block, which drives in situ self-assembly to form well-defined diblock copolymer spheres, worms, or vesicles. The final particle morphology obtained at full monomer conversion is dictated by (i) the target degree of polymerization of the PHPMA block and (ii) the total solids concentration at which the HPMA polymerization is conducted. Moreover, if the targeted diblock copolymer composition corresponds to vesicle phase space at full monomer conversion, the in situ particle morphology evolves from spheres to worms to vesicles during the in situ polymerization of HPMA. In the case of $PMPC_{25}$−$PHPMA_{400}$ particles, this systematic approach allows the direct, reproducible, and highly efficient preparation of either block copolymer vesicles at up to 25% solids or well-defined worms at 16−25% solids in aqueous solution.

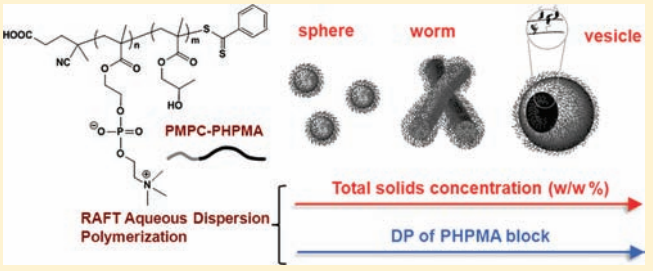

INTRODUCTION

Self-assembly of either AB diblock or ABC triblock copolymers to form spherical micelles, worms/rods, lamellae, toroids, vesicles, etc. is well-known in both the solid state and dilute solution.[1−11] Such polymeric nanostructures form the basis of so-called soft nanotechnology[12] and offer many applications as templates, coatings, and elastomers and also for nanomedicine.[13−16] In a selective solvent for one of the blocks, either micelles, worms, or vesicles are most commonly formed, depending on the relative volume fraction of the core-forming block.[7−11,17] Particularly in the case of vesicles, significant processing is often required, and such self-assembly can normally only be achieved in dilute solution (<1% solids). Although the basic design rules are well understood, producing worms in solution is rather problematic because this phase normally occupies a rather narrow region of the block copolymer phase diagram.[10] Here we show that AB diblock copolymer self-assembly can be precisely controlled by sequential reorganization during in situ polymerization in *concentrated* aqueous solution. The full sequence of phases is only observed by targeting sufficiently long core-forming blocks at sufficiently high concentration. This important advance is achieved using reversible addition−fragmentation chain transfer (RAFT) chemistry[18,19] to prepare AB diblock copolymers under aqueous dispersion polymerization conditions at 70 °C. A biocompatible poly(2-(methacryloyloxy)ethylphosphorylcholine) (PMPC)[20,21] chain transfer agent serves as the solvated "A" block. Chain extension of this zwitterionic block with 2-hydroxypropyl methacrylate in water produces a hydrophobic poly(2-hydroxypropyl methacrylate) (PHPMA) "B" block, which drives in situ self-assembly to form spheres, worms, or vesicles. A detailed phase diagram has been elucidated in which, for a given mean degree of polymerization (DP) of the PMPC block, the final particle morphology obtained at full conversion is solely dictated by (i) the target DP of the PHPMA block and (ii) the total solids concentration at which the HPMA polymerization is conducted. Moreover, if the final targeted phase is vesicles, the observed morphology *evolves* from spheres to worms to vesicles during the in situ polymerization of HPMA. Our approach is similar to the situation in nature, where lipids are produced in high concentrations to spontaneously form vesicles. Using the phase diagram as a predictive "roadmap" enables the direct,

Received: June 24, 2011
Published: August 19, 2011

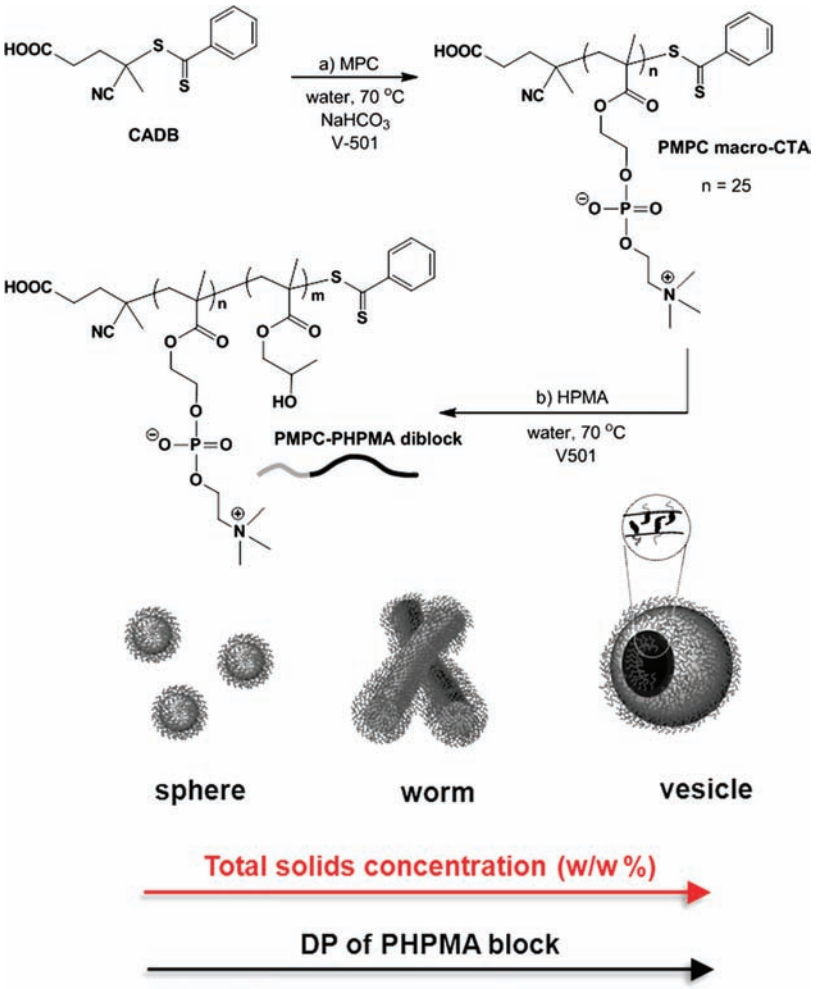

Figure 1. (a) Synthesis of the $PMPC_{25}$ macro-CTA via RAFT polymerization in aqueous solution and (b) RAFT aqueous dispersion polymerization of HPMA using this $PMPC_{25}$ macro-CTA at 70 °C. Using this facile approach, either spheres, worms, or vesicles can be directly prepared, depending on either the total solids concentration or the mean degree of polymerization of the PHPMA block.

reproducible, and highly efficient preparation of pure phases comprising either block copolymer vesicles at up to 25% solids or well-defined worms at 16−25% solids in aqueous solution. Such an efficient "polymerization-induced self-assembly" strategy is expected to provide new impetus to the field of block copolymers, as well as offer a range of potential commercial applications for such nanostructured materials.

An essential prerequisite for aqueous dispersion polymerization is a water-soluble monomer that forms a water-insoluble polymer. Herein this technique has been utilized to achieve in situ block copolymer self-assembly in aqueous solution. Thus, RAFT polymerization of 2-hydroxypropyl methacrylate (HPMA) was conducted in water using a PMPC-based chain transfer agent (CTA) (Figure 1). As the PHPMA chains grow, they become increasingly hydrophobic. Thus, the resulting PMPC−PHPMA block copolymers undergo spontaneous self-assembly in water. The final particle morphology is controlled not only by the PMPC/PHPMA block ratio but also by the total solids concentration under which the HPMA polymerization is conducted. Thus, by fixing the mean DP of the PMPC chains, we have constructed a detailed phase diagram for the three block copolymer morphologies (spheres, worms, or vesicles) simply by varying two synthesis parameters: the target DP of the PHPMA chains and the total solids concentration.

RESULTS AND DISCUSSION

First, we prepared near-monodisperse $PMPC_{25}$ homopolymer using 4,4′-azobis(4-cyanopentanoic acid) (V-501) initiator and 4-cyanopentanoic acid dithiobenzoate (CADB) as a RAFT chain transfer agent in water in the presence of $NaHCO_3$. The latter reagent was simply used to adjust the pH and hence improve the water solubility of the CADB. RAFT polymerization proceeded smoothly at approximately pH 8 and was almost complete after 2 h (Figure S1a in the Supporting Information). The mean DP of the resulting PMPC homopolymer was determined by ^{1}H NMR spectroscopy. The actual DP of 25 estimated from the aromatic RAFT end group was in good agreement with the targeted DP, and the final copolymer polydispersity was relatively narrow as judged by gel permeation chromatography (GPC) (Figures S1b, S2, and S3, Supporting Information). This $PMPC_{25}$ homopolymer was then used as a so-called "macro-CTA" for the second-stage RAFT aqueous dispersion polymerization of HPMA.

Using the same $PMPC_{25}$ macro-CTA, we prepared various $PMPC_{25}$−$PHPMA_x$ diblock copolymers directly in water while also varying the total solids content of the formulation. The combined mass of HPMA and $PMPC_{25}$ macro-CTA (the mass of the free radical initiator is considered negligible) was initially

Table 1. Molecular and Morphological Characterization of $PMPC_{25}$−$PHPMA_x$ Diblock Copolymers Prepared by RAFT Dispersion Polymerization in Water at 70 °C[a]

sample code[b]	solids content (wt %)[c]	N_{PHPMA}[d]	W_{PMPC}[e]	M_n[f] (kg/mol)	PDI[f]	morphology[g]
$M_{25}H_{100}$-10	10.0	98	0.34	21.4	1.23	S
$M_{25}H_{100}$-15	15.0	101	0.34	22.0	1.27	S
$M_{25}H_{100}$-20	20.0	100	0.34	22.6	1.27	S
$M_{25}H_{100}$-25	25.0	99	0.34	23.0	1.23	S
$M_{25}H_{150}$-10	10.0	152	0.25	39.9	1.23	S
$M_{25}H_{150}$-15	15.0	151	0.25	39.8	1.24	S
$M_{25}H_{150}$-20	20.0	152	0.25	38.5	1.25	S
$M_{25}H_{150}$-25	25.0	148	0.26	37.1	1.22	S
$M_{25}H_{200}$-10	10.0	200	0.20	58.0	1.36	S
$M_{25}H_{200}$-15	15.0	201	0.20	53.0	1.35	S
$M_{25}H_{200}$-20	20.0	202	0.20	57.5	1.38	S
$M_{25}H_{200}$-25	25.0	207	0.20	51.0	1.33	S, W
$M_{25}H_{220}$-25	25.0	220	0.19	59.9	1.38	W
$M_{25}H_{250}$-10	10.0	251	0.17	68.2	1.27	S
$M_{25}H_{250}$-13	13.0	255	0.17	66.5	1.26	S
$M_{25}H_{250}$-15	15.0	251	0.17	70.1	1.29	S, W
$M_{25}H_{250}$-20	20.0	256	0.17	69.9	1.29	S, W
$M_{25}H_{275}$-25	25.0	278	0.16	72.0	1.29	W
$M_{25}H_{300}$-10	10.0	301	0.15	94.4	1.56	S
$M_{25}H_{300}$-15	15.0	294	0.15	97.6	1.49	S, W
$M_{25}H_{300}$-20	20.0	298	0.15	86.4	1.50	S, W
$M_{25}H_{300}$-25	25.0	299	0.15	99.9	1.48	W, V
$M_{25}H_{320}$-25	25.0	321	0.14	110.0	1.56	W, V
$M_{25}H_{350}$-10	10.0	354	0.13	132.2	1.42	S
$M_{25}H_{350}$-15	15.0	351	0.13	125.1	1.44	S, W
$M_{25}H_{350}$-20	20.0	349	0.13	124.0	1.46	W
$M_{25}H_{370}$-25	25.0	372	0.12	142.4	1.61	V
$M_{25}H_{400}$-10	10.0	397	0.11	171.9	1.67	S
$M_{25}H_{400}$-12.5	12.5	395	0.11	173.2	1.73	S, W
$M_{25}H_{400}$-15	15.0	401	0.11	185.6	1.66	S, W
$M_{25}H_{400}$-16.2	16.2	399	0.11	174.3	1.38	W
$M_{25}H_{400}$-17.5	17.5	399	0.11	181.4	1.39	W, V
$M_{25}H_{400}$-20	20.0	401	0.11	172.6	1.69	W, V
$M_{25}H_{400}$-22.5	22.5	398	0.11	176.3	1.51	V
$M_{25}H_{400}$-23	23.0	401	0.11	173.0	1.71	V
$M_{25}H_{400}$-25	25.0	398	0.11	172.0	1.70	V

[a] All these entries were used to construct the phase diagram shown in Figure 3: $PMPC_{25}$ macro-CTA (0.25 g, 0.0326 mmol), [$PMPC_{25}$ macro-CTA]$_0$/[V-501]$_0$ = 4.0, polymerization time 20 h. [b] The individual PMPC and PHPMA blocks are denoted by M and H, respectively. [c] [$PMPC_{25}$ macro-CTA (g) + HPMA (g)]/[all reaction mixtures (g)] × 100. [d] Determined by ^{1}H NMR spectroscopy in d_4-methanol, assuming that the blocking efficiency of the $PMPC_{25}$ macro-CTA is 100%: conversion >99%. [e] Weight fraction of the PMPC block in the particle. [f] Polydispersity index. Determined by GPC [poly(methyl methacrylate) (PMMA) standards, 3:1 $CHCl_3$/methanol eluent with 2 mM LiCl]. [g] Copolymer morphologies formed in water identified using TEM and tapping-mode AFM: S = spheres, W = worms, and V = vesicles. Coexisting phases are indicated by two letters, where appropriate.

fixed at 10 wt %. We use the copolymer notation $M_{25}H_m$-*Y*, where M stands for PMPC, H stands for PHPMA, *m* is the target DP of the PHPMA block in each case, and *Y* denotes the total solids content used for each formulation. Both the $PMPC_{25}$ macro-CTA and the HPMA monomer are initially fully soluble in the aqueous reaction solution, but the aqueous dispersion polymerization of HPMA leads to in situ phase separation and self-assembly, with the final morphology of the $PMPC_{25}$−$PHPMA_m$ diblock copolymer particles dictated solely by the initial reaction conditions. Very high HPMA conversions are observed within 2 h, as judged by ^{1}H NMR spectroscopy. The $PMPC_{25}$−$PHPMA_x$ diblock copolymer molecular weight distribution is shifted to significantly higher molecular weight relative to the $PMPC_{25}$ macro-CTA, with little evidence for any unreacted PMPC homopolymer, regardless of the target block composition (see Figure S3, Supporting Information). However, there is a prominent high molecular weight shoulder, particularly if targeting higher DP PHPMA chains. This is due to a small amount (∼0.26 mol %) of dimethacrylate impurity known to be present in HPMA monomer.[22] However, this impurity causes relatively light branching rather than cross-linking, since no $PMPC_{25}$−$PHPMA_x$ diblock copolymer particles can be detected in methanol (which is a good solvent for both the PMPC and PHPMA blocks) as judged by dynamic light scattering. All polymerization

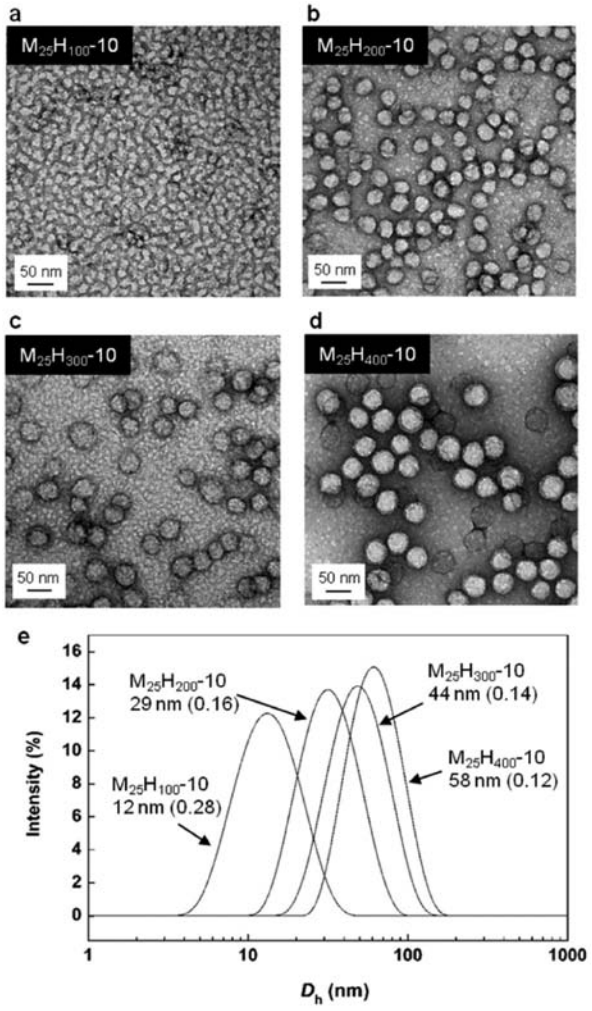

Figure 2. TEM images obtained for a series of $M_{25}H_m$-10 diblock copolymer spheres prepared by RAFT aqueous dispersion polymerization at 70 °C (here "10" denotes a total solids content of 10 wt %): (a) $M_{25}H_{100}$-10, (b) $M_{25}H_{200}$-10, (c) $M_{25}H_{300}$-10, and (d) $M_{25}H_{400}$-10. In each case the PMPC block length is fixed and the PHPMA block length is systematically varied. (e) DLS particle size distributions (intensity vs mean hydrodynamic diameter, D_h) obtained for the same series of diblock copolymer spheres, $M_{25}H_m$-10 (m = 100−400). The inset values indicate the mean diameter and polydispersity index (in parentheses) for each sample, as calculated by cumulants analysis.

data are summarized in Table 1. A representative transmission electron microscopy (TEM) image and dynamic light scattering (DLS) results for various $PMPC_{25}$−$PHPMA_x$ diblock copolymer particles ($M_{25}H_{100}$-10, $M_{25}H_{200}$-10, $M_{25}H_{300}$-10, and $M_{25}H_{400}$-10) are shown in Figure 2. A systematic increase in the target DP of the PHPMA block from 100 to 400 leads to a monotonic increase in the intensity-average particle diameter from 12 to 58 nm, as judged by DLS. In each case TEM studies indicated exclusively spherical particle morphologies, and number-average diameters estimated from TEM studies were consistent with the DLS data.

^{1}H NMR spectra were recorded for the $PMPC_{25}$ macro-CTA dissolved in D_2O, a RAFT-synthesized $PHPMA_{50}$ homopolymer control in d_4-methanol and $M_{25}H_m$-10 (m = 100−400) particles redispersed in both D_2O and d_4-methanol (see Figures S4 and S5, respectively, Supporting Information). All the signals associated with the $PMPC_{25}$ macro-CTA are observed in each of the spectra recorded in D_2O. However, none of the PHPMA signals are visible in this solvent, regardless of the PHPMA block length. In contrast, all the signals expected for the PMPC and PHPMA blocks are visible in the spectra recorded in d_4-methanol. Thus, these NMR observations suggest that the $PMPC_{25}$ chains act as the solvated steric stabilizer, while the PHPMA chains form the nonsolvated nanolatex cores.

Dramatic changes in block copolymer morphology were observed when the aqueous dispersion polymerization of HPMA was conducted under increasingly concentrated conditions. For example, spheres, worms, or vesicles were observed for the $M_{25}H_{400}$-Y series: spheres were obtained at Y = 10%, both spheres and worms were obtained at 12.5% and 15%, a pure worm phase was obtained at 16.2%, both worms and vesicles were obtained at 17 and 20%, and purely vesicles were obtained for $Y \geq$ 22.5% (see Figure 3 and Table 1). For a given block copolymer, the morphology formed in solution depends on the relative pervaded volumes and cross-sectional areas of the chains that dictate the interfacial curvature. Given that PHPMA is hydrophobic, its volume is not particularly affected by the concentration, whereas the pervaded volume of the PMPC chain is sensitive to its solvation. Previously, Ishihara[23] has reported that each MPC repeat unit is associated with up to 24 water molecules. Thus, an increase in copolymer concentration reduces the activity of the water and causes a reduction in the pervaded volume of the PMPC block. In dilute solution the interfacial curvature is concave with respect to PMPC, which leads to micelles, whereas in the bulk the spontaneous curvature of $M_{25}H_{400}$ is convex, forming PMPC spheres in a PHPMA matrix. At some intermediate concentration, the interfaces are essentially flat and vesicles form. Varying the target DP of the PHPMA block at a fixed Y = 25% leads to similar morphological control. Thus, for the $M_{25}H_m$-25 series, pure phases of spheres, worms, or vesicles were observed for m = 150, 275, and 400, respectively. All of our morphological observations are summarized in the form of a detailed phase diagram shown in Figure 3. Using uranyl formate as a negative stain, five distinct phases have been identified by TEM (see Figure S6, Supporting Information, for further TEM images relating to Figure 3). For HPMA polymerizations conducted at relatively high concentration, a pure vesicle phase was observed when targeting a high DP (e.g., $M_{25}H_{400}$-25, average diameter 140 nm by TEM, D_h = 186 nm (PDI = 0.18) by DLS; see Figure 3 and Figure S7, Supporting Information). These vesicles were also examined after drying from dilute aqueous solution onto a mica substrate using atomic force microscopy (AFM). The average vesicle diameter of 145 nm agrees well with TEM data (see Figure S8, Supporting Information). More importantly, the hollow nature of such vesicles was confirmed, since the height of the central domain was much lower than that at the edge. However, the average vesicle dimensions determined by TEM and AFM were somewhat lower than the hydrodynamic diameters reported by DLS, since the latter technique is sensitive to both hydration and polydispersity.

Close inspection of the various worm phases observed by TEM for $M_{25}H_{220}$-25, $M_{25}H_{275}$-25, $M_{25}H_{350}$-20, and $M_{25}H_{400}$-16.2 indicated mean "inner core" (i.e., PHPMA block only) worm widths of 22, 26, 35, and 41 nm, respectively, with worm lengths exceeding 1 μm in most cases (see Figure 3 and Figure S6, Supporting Information). Thus, the inner core worm width varies monotonically with the DP of the core-forming PHPMA chains, as expected. These TEM observations are also consistent

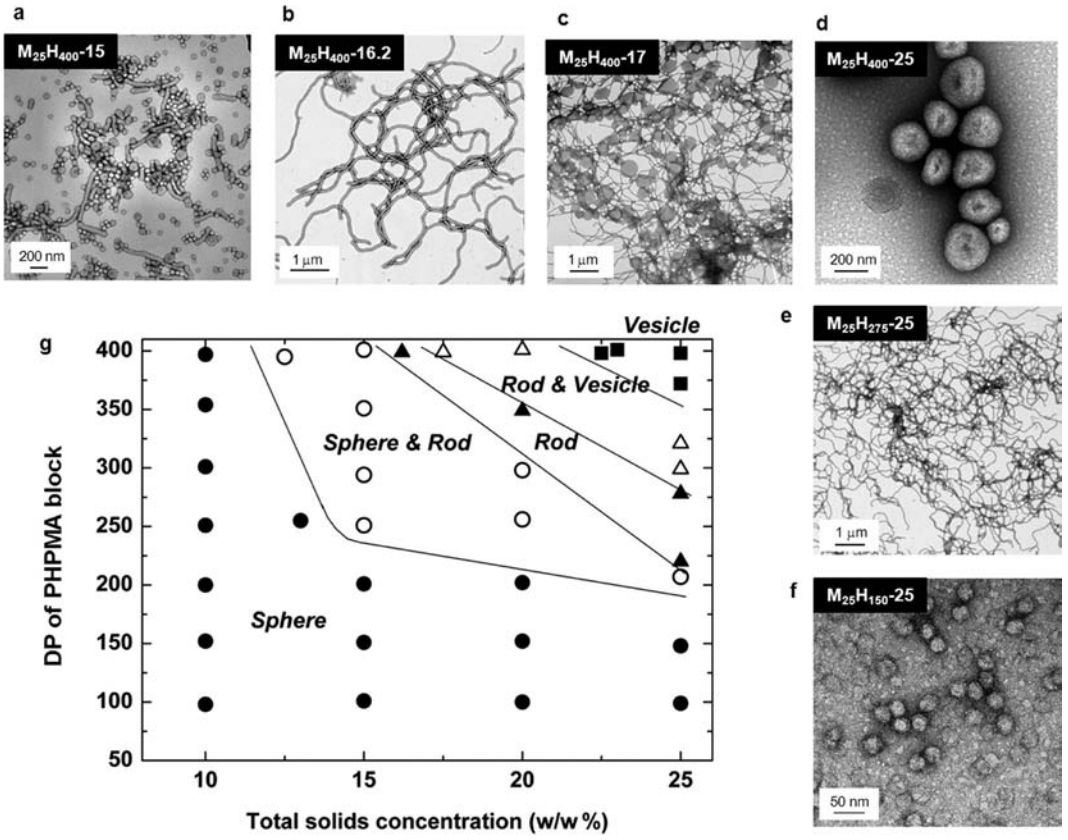

Figure 3. Detailed phase diagram constructed for the $M_{25}H_x$-*Y* formulation (where M denotes MPC and H denotes HPMA) by systematic variation of the mean target degree of polymerization of PHPMA (*x*) and the total solids concentration (*Y*) used for each synthesis. The mean DP values of the PHPMA block shown in the phase diagram were calculated from the diblock copolymer composition determined by ^{1}H NMR spectroscopy in d_4-methanol assuming 100% blocking efficiency for the $PMPC_{25}$ macro-CTA. (a–f) TEM images for representative morphologies: (a) $M_{25}H_{400}$-15 (spheres and worms), (b) $M_{25}H_{400}$-16.2 (worms), (c) $M_{25}H_{400}$-17 (worms and vesicles), and (d) $M_{25}H_{400}$-25 (vesicles), i.e., identical diblock copolymers prepared at differing copolymer concentrations. (e) $M_{25}H_{275}$-25 and (f) $M_{25}H_{150}$-25 are two other diblock copolymers prepared at the same 25 wt % solids content used for image d.

with our AFM data (see Figure S9, Supporting Information). The mean worm core widths were estimated from TEM images and plotted against the mean DP of the core-forming PHPMA block (Figure 4). These data can be fitted to a power law that relates the core diameter, *d*, to the mean DP of the hydrophobic PHPMA blocks, *N*, such that $d = kN^{\alpha}$, where *k* is a constant that depends on the Flory–Huggins parameter and *N* scales with an exponent α of 1 (within experimental error).[24] This indicates that the PHPMA chains within the worms are fully extended. In contrast, the α value obtained for a series of $PMPC_{25}$–$PHPMA_x$ diblock copolymer spheres is approximately 0.78, which suggests that the conformation of the PHPMA chains is intermediate between the fully stretched and fully collapsed states. These exponents are consistent with those reported by Förster et al.[25] Furthermore, DLS studies indicate that these diblock copolymer worms give rise to more intense light scattering and significantly larger "sphere-equivalent" diameters than the block copolymer spheres and vesicles (Figure S7, Supporting Information). As-synthesized worm phases such as $M_{25}H_{400}$-22.5 and $M_{25}H_{350}$-25 were sufficiently viscous to cause physical gelation, as judged by the tube inversion method. Previously, both block copolymer worms/fibers and vesicles have been reported by Pan et al.[26] and Charleux et al.[27] using either alcoholic dispersion or aqueous emulsion polymerization. We have recently described many examples of diblock copolymer spheres (termed "nanolatexes") and also a single example of a block copolymer vesicle via aqueous dispersion polymerization.[28] However, these literature examples were simply achieved by varying the diblock copolymer composition: as far as we are aware, the effect of varying the total solids concentration has not been properly explored for such RAFT syntheses. An important aspect of the present study is the recognition that, for RAFT aqueous dispersion polymerization, varying the total solids concentration offers a second highly effective means of tuning the diblock copolymer morphology, since this insight allows the construction of a *predictive* phase diagram for a given diblock copolymer formulation.

The zwitterionic nature of the PMPC chains effectively shields any underlying surface charge, leading to a relatively flat ζ potential vs pH curve for the PMPC–PHPMA diblock copolymer particles, regardless of their morphology (see Figure 5). As discussed above, the PMPC–PHPMA worm phase readily forms soft, free-standing gels in aqueous solution while in principle the PMPC–PHPMA vesicles can encapsulate various actives such as dyes. Given that such block copolymers are efficiently prepared directly in water and have already been demonstrated to be both highly biocompatible[29] and also antibacterial,[30] these novel nanoparticles may have interesting biomedical applications.

Formulations that produce pure vesicle and worm phases such as $M_{25}H_{400}$-25 and $M_{25}H_{275}$-25 were dissolved in methanol

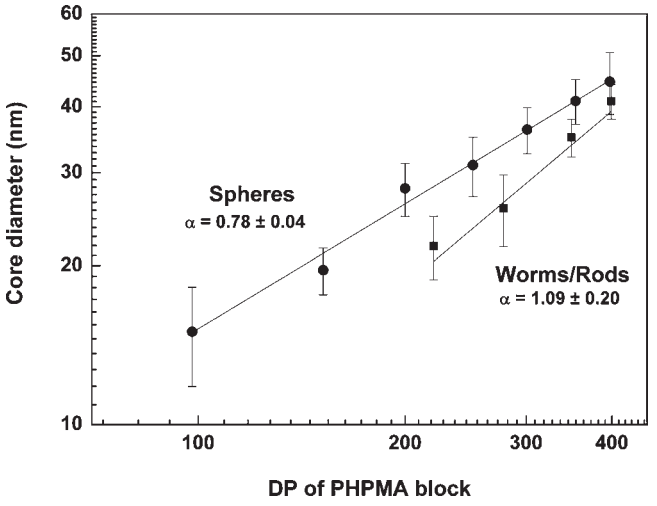

Figure 4. Relationship between inner core diameter and DP of PHPMA for spheres and worms. A power law of the form $d = kN^{\alpha}$ can be plotted, and scaling powers of $\alpha = 0.78 \pm 0.04$ and 1.09 ± 0.20 are calculated for spheres and worms, respectively. For spheres, the $M_{25}H_m$-10 series was used. For worms, we used the $M_{25}H_{220}$-25, $M_{25}H_{275}$-25, $M_{25}H_{350}$-20, and $M_{25}H_{400}$-16.2 series.

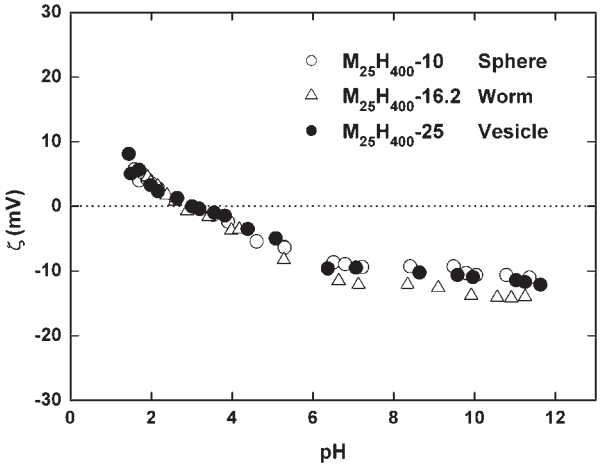

Figure 5. ζ potential vs pH curves for dilute (0.1 g/L) aqueous solutions of $M_{25}H_{400}$-*Y* particles with the following morphologies: (○) spheres, $M_{25}H_{400}$-10; (△) worms, $M_{25}H_{400}$-16.2; (●) vesicles, $M_{25}H_{400}$-25.

(which is a good solvent for both blocks) and then dialyzed against water. Intriguingly, their original morphologies were lost, and purely spherical phases were obtained, as judged by TEM (see Figure S10, Supporting Information). Moreover, DLS studies indicate that the spherical diameter of 55 nm obtained for $M_{25}H_{400}$-25 after this processing step corresponds closely to that observed for the same diblock copolymer prepared at 10 wt % solids in water (53 nm). On the other hand, mere *dilution* of the $M_{25}H_{400}$-25 vesicles (or $M_{25}H_{275}$-25 worms) with water did not lead to any change in the block copolymer morphology. These results suggest that our in situ self-assembly synthetic route produces frozen, nonergodic structures in aqueous solution, as expected.

For pseudoliving polymerizations such as RAFT, it is well-known that the molecular weight of the polymer chains increases

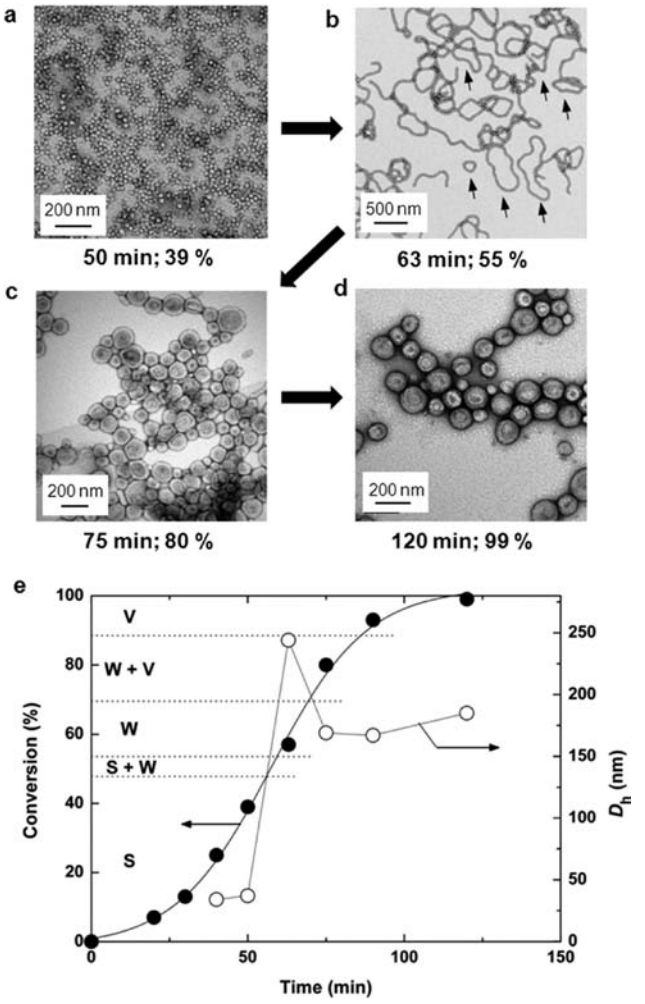

Figure 6. Morphological changes that occur during aqueous dispersion polymerization. TEM images of the various block copolymer morphologies obtained after specific polymerization times when targeting a final block copolymer with an $M_{25}H_{400}$-25 composition: (a) 50 min, 39% conversion (spheres), (b) 63 min, 55% conversion (worms or toroids and loops; see arrows), (c) 75 min, 80% conversion (worms and vesicles), and (d) 120 min, 99% conversion (vesicles). (e) Kinetic data for the targeted $M_{25}H_{400}$-25 composition at 70 °C and the DLS hydrodynamic particle diameter (D_h) as a function of the polymerization time. The separate phase regions are estimated from a series of $M_{25}H_m$-25 syntheses (see the phase diagram shown in Figure 3): S = spheres, W = worms, and V = vesicles. Polymerization conditions: $PMPC_{25}$ macro-CTA (0.250 g, equivalent to 0.847 mmol of MPC repeat units), HPMA (1.954 g, 13.552 mmol; target DP 400), V-501 initiator (2.3 mg, 0.0082 mmol; CTA/initiator molar ratio 4.0), and water (6.610 g).

linearly with conversion.[19,20] Thus, during the aqueous dispersion polymerization of HPMA via RAFT, the mean DP of all the PHPMA chains gradually increases. However, as we have seen, this DP is a critical parameter in determining the block copolymer morphology. If a relatively high final DP is targeted to produce a purely vesicular phase (e.g., $M_{25}H_{400}$-25; see Figure 3), then in principle all the various block copolymer phases should be generated in situ *during the HPMA polymerization*. Thus, the synthesis of $M_{25}H_{400}$-25 was revisited in a detailed kinetic study; see Figure 6 (for the evolution of M_n and M_w/M_n with conversion, see Figure S11, Supporting Information). Initially, the reaction solution was transparent. However, as the polymerization

proceeded, the aqueous phase gradually became more turbid (the pink color derived from the RAFT CTA was retained) and the solution viscosity increased, passing through a maximum after around 60−65 min as the PHPMA chains continued to grow (Figure S12, Supporting Information); the HPMA polymerization was essentially complete within 2 h. TEM studies confirmed that the block copolymer morphology changed from spheres to worms to vesicles during the HPMA polymerization, as expected. Moreover, if the monomer conversion obtained by NMR at any given time is used to estimate the mean DP for the PHPMA block, then the block copolymer morphology observed by TEM corresponds to that expected from the phase diagram shown in Figure 3; thus, the cosolvent effect of the HPMA monomer on the block copolymer morphology is negligible. Finally, for the worm phase observed after 63 min (conversion 55%, which approximately corresponds to $M_{25}H_{220}$ on the basis of ^{1}H NMR spectroscopy), the mean TEM worm core width was 21 nm.

In summary, we have elucidated the first phase diagram for polymerization-induced self-assembly using living radical polymerization. This can be used to *predict* pure phase regions and hence enables the facile, efficient, and reproducible preparation of spheres, worms, or vesicles *directly in concentrated aqueous solution*. This systematic approach is a significant improvement on the ad hoc strategies previously reported and is expected to transform the availability of well-defined worm and vesicle phases for characterization studies.

■ ASSOCIATED CONTENT

Supporting Information. Full Experimental Section and further synthesis and characterization details for the PMPC-PHPMA block copolymers using GPC, ^{1}H NMR, DLS, TEM, and AFM. This material is available free of charge via the Internet at http://pubs.acs.org.

■ AUTHOR INFORMATION

Corresponding Author
sugihara@u-fukui.ac.jp; s.p.armes@sheffield.ac.uk

■ ACKNOWLEDGMENT

Biocompatibles is thanked for supplying the MPC monomer and for permission to publish this work. Dr. Zhenyu Zhang is thanked for his assistance with the AFM studies.

■ REFERENCES

(1) Hillmyer, M. A.; Bates, F. S.; Almdal, K.; Mortensen, K.; Ryan, A. J.; Fairclough, J. P. A. *Science* **1996**, *271*, 976–978.
(2) Wang, X.; Guerin, G.; Wang, H.; Wang, Y.; Manners, I.; Winnik, M. A. *Science* **2007**, *317*, 644–647.
(3) Cui, H.; Chen., Z.; Zhong, S.; Wooley, K. L.; Pochan, D. J. *Science* **2007**, *317*, 647–650.
(4) Pochan, D. J.; Chen, Z.; Cui, H.; Hales, K.; Qi, K.; Wooly, K. L. *Science* **2004**, *306*, 94–97.
(5) Hawker, C. J.; Wooley, K. L. *Science* **2005**, *309*, 1200–1205.
(6) Won, Y.-Y.; Davis, H. T.; Bates, F. S. *Science* **1999**, *283*, 960–963.
(7) Discher, D. E.; Eisenberg, A. *Science* **2002**, *297*, 967–973.
(8) Zhang, L.; Yu, K.; Eisenberg, A. *Science* **1996**, *272*, 1777–1779.
(9) Zhang, L.; Eisenberg, A. *Science* **1995**, *268*, 1728–1731.
(10) Jain, S.; Bates, F. S. *Science* **2003**, *300*, 460–464.
(11) Discher, B. M.; Won, Y.-Y.; Ege, D. S.; Lee, J. C.-M.; Bates, F. S.; Discher, D. E.; Hammer, D. A. *Science* **1999**, *284*, 1143–1146.
(12) Hamley, I. W. *Angew. Chem., Int. Ed.* **2003**, *42*, 1692–1712.
(13) Arsenault, A. C.; Rider, D. A.; Tértreault, N.; Chen, J. I.-L.; Coombs, N.; Ozin, G. A.; Manners, I. *J. Am. Chem. Soc.* **2005**, *127*, 9954–9955.
(14) Howse, J. R.; Jone, R. A; Battaglia, G.; Ducker, R. E.; Leggett, G. J. *Nat. Mater.* **2009**, *8*, 507–511.
(15) Cheng, J. Y.; Mayes, A. M.; Ross, C. A. *Nat. Mater.* **2004**, *3*, 823–828.
(16) Savić, R.; Luo, L.; Eisenberg, A.; Maysinger, D. *Science* **2003**, *300*, 615–618.
(17) Antonietti, M.; Förster, S. *Adv. Mater.* **2003**, *15*, 1323–1332.
(18) Chiefari, J.; Chong, Y. K.; Ercole, F.; Krstina, J.; Jeffery, J.; Le, T. P. T.; Mayadunne, R. T. A.; Meijs, G. F.; Moad, C. L.; Moad, G.; Rizzard, E.; Thang, S. H. *Macromolecules* **1998**, *31*, 5559–5562.
(19) (a) Moad, G.; Rizzardo, E.; Thang, S. H. *Aust. J. Chem.* **2005**, *58*, 379–410. (b) Moad, G.; Rizzardo, E.; Thang, S. H. *Polymer* **2008**, *49*, 1079–1131.
(20) Lobb, E. J.; Ma, I.; Billingham, N. C.; Armes, S. P. *J. Am. Chem. Soc.* **2001**, *123*, 7913–7914.
(21) Du, J.; Tang, Y.; Lewis, A. L.; Armes, S. P. *J. Am. Chem. Soc.* **2005**, *127*, 17982–17983.
(22) Ali, A. M. I.; Pareek, P.; Sewell, L.; Schmid, A.; Fujii, S.; Armes, S. P. *Soft Matter* **2007**, *3*, 1003–1013.
(23) Morisaku, T.; Watanabe, J.; Konno, T.; Takai, M.; Ishihara, K. *Polymer* **2008**, *49*, 4652-4657.
(24) Battaglia, G.; Ryan, A. J. *J. Am. Chem. Soc.* **2005**, *127*, 8757–8764.
(25) Förster, S.; Plantenberg, T. *Angew. Chem., Int. Ed.* **2002**, *41*, 688–714.
(26) (a) Wan, W.-M.; Hong, C.-Y.; Pan, C.-Y. *Chem. Commun.* **2009**, 5883–5885. (b) Wan, W.-M.; Sun, X.-L.; Pan, C.-Y. *Macromolecules* **2009**, *42*, 4950–4952. (c) Cai., W.; Wan, W.; Hong, C.; Huang, C.; Pan., C. *Soft Matter* **2010**, *6*, 5554–5561. (d) He, W.-D.; Sun, X.-L.; Wan, W.-M.; Pan, C.-Y. *Macromolecules* **2011**, *44*, 3358–3365.
(27) (a) Delaittre, G.; Dire, C.; Rieger, J.; Putaux, J.-L.; Charleux, B. *Chem. Commun.* **2009**, 2887–2889. (b) Boissé, S.; Rieger, J.; Belal, K.; Di-Cicco, A.; Beaunier, P.; Li, M. H.; Charleux, B. *Chem. Commun.* **2010**, *46*, 1950–1952. (c) Zhang, X.; Boissé, S.; Zhang, W.; Beaunier, P.; D'Agosto, F.; Rieger, J.; Charleux, B. *Macromolecules* **2011**, *44*, 4149–4158. (d) Boissé, S.; Rieger, J.; Pembouong, G.; Beaunier, P.; Charleux, B. *J. Polym. Sci., Part A: Polym. Chem.* **2011**, *49*, 3346–3354.
(28) Li, Y.; Armes, S. P. *Angew. Chem., Int. Ed.* **2010**, *49*, 4042–4046.
(29) Madsen, J.; Armes, S. P.; Bertal, K.; Lomas, H.; MacNeil, S.; Lewis, A. L. *Biomacromolecules* **2008**, *9*, 2265–2275.
(30) Bertal, K.; Shepherd, J.; Ian Douglas, C. W.; Madsen, J.; Morse, A.; Edmondson, S.; Armes, S. P.; Lewis, A.; MacNeil, S. *J. Mater. Sci.* **2009**, *44*, 6233–6246.